Spectral Sensitivity of Simulated Photovoltaic Module Soiling for a Variety of Synthesized Soil Types

Patrick D. Burton and Bruce H. King, *Member, IEEE*

***Abstract*—The accumulation of soil on photovoltaic (PV) modules may introduce a spectral loss due to the color profile of the accumulated material. In order to compare the spectral and total losses experienced by a cell, soil analogs were formulated to contain common mineral pigments (Fe_2O_3 and göthite) with previously developed "standard grime" mixtures. These mixtures simulated a wide range of desert soil colors and were applied to glass test coupons. The light transmission through the deposited film was evaluated by UV/vis/NIR spectroscopy and by placing the coupon over a test cell in a 1-sun simulator and quantum efficiency test stand. Distinct peaks in the 300–600-nm range were observed by UV/vis/NIR spectroscopy corresponding to the Fe_2O_3 and göthite. Approximately analogous features were noted in the QE measurement. Overall comparisons were made by integrating the response of a soiled coupon relative to a clean reference. Soils rich in red pigments (Fe_2O_3) caused a greater integrated response than soils rich in yellow pigment (göthite). The yellow soils caused a greater attenuation in a specific region of the spectrum (300–450 nm), which may have significant implications to specific devices, such as multijunction and CdTe technologies.**

***Index Terms*—Performance evaluation, photovoltaic (PV) systems, soil coatings. standardized test methods, surface contamination.**

I. Introduction

THE study of soil accumulation on photovoltaic (PV) surfaces has been of interest for nearly 70 years [1]. However, controllable investigations of the effects of soil on glass and reflective surfaces for the PV and concentrating solar power (CSP) communities are limited. Specifically, predicting the loss due to accumulated soiling could be a valuable tool to system planners and operators. Such losses are difficult to predict without previous knowledge of the soil type and accumulation patterns in a selected area. Previous work [2] has shown that accelerated soiling methods can be used to evaluate the response of soil in a controlled laboratory setting.

Manuscript received October 22, 2013; revised December 19, 2013; accepted January 14, 2014. Date of publication February 5, 2014; date of current version April 18, 2014. This work was supported by the U.S. Department of Energy SunShot Initiative under LPDP Agreement 25800. Sandia National Laboratories is a multiprogram laboratory managed and operated by Sandia Corporation, a wholly owned subsidiary of Lockheed Martin Corporation, for the U.S. Department of Energy's National Nuclear Security Administration under contract DE-AC04-94AL85000.

The authors are with Sandia National Laboratories, Albuquerque, NM 87123 USA (e-mail: pdburto@sandia.gov; bhking@sandia.gov).

Color versions of one or more of the figures in this paper are available online at http://ieeexplore.ieee.org.

Digital Object Identifier 10.1109/JPHOTOV.2014.2301895

In order to effectively predict the decrease in the performance of a PV installation, it is necessary to have a reasonable estimate of the extent of soiling in the region. Cattle *et al.* [3] have shown that dust accumulation can vary significantly within a single area due to a point source. This level of detail can be useful for a planned installation; however, the data in this study took several years to collect. A faster testing and evaluation method would be valuable to assist in locating, sizing, and installing a PV facility. Specific knowledge of the interaction between accumulated soil and the incident light would assist in these predictions.

The loss due to soiling experienced by PV modules is primarily due to the interception of the incident light by surface contaminants. However, each particle does not directly correlate with a missed opportunity for the device to collect the light. Forward scattering through soil films has been discussed by Biryukov *et al.* [4]. The reduction in the short-circuit current was not proportional to the measured soil area coverage. The light that had scattered around the accumulated particles was still able to reach the test device.

Additionally, the type of soil may influence the spectral content of the incident light. This is especially important to research and development efforts attempting to collect a wider fraction of the available spectrum. For example, recent enhancements in organic PV cells have been demonstrated [5] by coupling spectrally sensitive layers to enhance collection up to 900 nm. Since the energy of the incident spectrum at 900 nm is roughly half that at 600 nm, any losses due to soiling would be very significant to these carefully designed devices. Understanding the loss due to soiling could offer useful insight to the design, manufacture, and cost-effective deployment of these types of cells. Wavelength dependence has also been considered for PV on Martian landers, as the Martian soil readily reflects the red light [6]. Single scattering was not considered to be significant, although the author did note that the available data were not sufficient to extend the analysis to a broader spectrum. Other work has investigated the effect of specific soil components on the response of outdoor PV systems [7].

In this paper, we expand upon a technique reported at the 39th Photovoltaics Specialists Conference [8] to systematically inspect the effect of soil color on the light transmission through glass coupons using an artificial soil termed "grime." In this paper, we build upon the prior work to include reflectance measurements and expanded discussion of specific soil effects. As before, the term grime will be used throughout this paper to refer to the laboratory-blended material. "Soil" will denote naturally occurring material and the accumulation thereof. Specifically,

the spectral effects of each grime have been evaluated with regard to direct illumination, scattered light, and overall impact on the cell performance. Levinson *et al.* [9] have noted previously that light scattering measurements on soiled surfaces are difficult. Our efforts reported herein have focused on the sensitivity of PV cells to the variation in soil color as a first-order approximation of various soils throughout the desert southwest United States. The pigmented grime in this paper has been compared with more generic grime formulas from earlier work [2] to establish the relative significance of location-specific blends. While this paper is by no means an exhaustive effort to quantify the behavior of all possible soil types, useful information has been gleaned by a systematic study of common soil pigments.

II. Experimental Methods

A. Grime Formulation

Grime mixtures were formulated according to a previously reported method [2], [10]. Briefly, a graded quartz sand (Arizona Road Dust, 0–80 μm) was mixed with a mineral pigment and a trace soot component. Arizona road dust (ISO 12103-1 A2 Fine Test Dust, Powder Technology Inc.) was mixed with a soot mixture composed of 83.3% w/w carbon black (Vulcan XC-723, Cabot); 8.3% diesel particulate matter (NIST Catalog No. 2975); 4.2% unused SAE 10W30 motor oil (Power Care); 4.2% α-pinene (Catalog No. AC13127-2500, Acros Organics) in a glass jar and tumbled without milling media in a rubber ball mill drum at 150 r/min for 48 to 72 h. Variations in grime composition were produced by incorporating major optical components into the base grime mixture. Naturally occurring iron oxides have been identified as common spectrally active components in atmospheric aerosols [11] and desert soils [12]. In this study, commercial Fe_2O_3 (99.98% trace metals basis, Sigma Aldrich) and in-house synthesized göthite [FeO(OH)] were incorporated as the primary red and yellow spectral components, respectively. For clarity, the commercial material will be referred to by the chemical name, while the house-synthesized göthite will be referred to by the mineral name. Dry grime mixtures were matched to Munsell color charts to easily compare with values reported in the literature [12], [13].

Göthite was produced following the procedure outlined by Schwertmann and Cornell [14, p. 78]. Briefly, 0.05 mol (9.9405 g) $FeCl_2 \cdot 4H_2O$ (Certified grade, Fisher) was dissolved in 1 L of DI H_2O that had been degassed by bubbling N_2 for 30 min. The solution was buffered with 110 mL of 1M $NaHCO_3$ (Enzyme grade, Fisher) and allowed to stir for up to 48 h. The resulting product was filtered and rinsed in DI H_2O and allowed to dry prior to analysis. The dried product was analyzed by X-ray diffraction (XRD) with a Bruker D8 Advance diffractometer that was operated at 40 kV and 30 mA. The scan was collected from 20 to 90° at a rate of 0.02° per step with a 2-s count time using a rotating sample holder. Bulk powder was color-matched to Munsell swatch 10 YR 5.5/8.

Grime blends were prepared by mixing 40 wt% of the desired pigment with 59.9 wt% AZ road dust and 0.1 wt% soot mixture. Specific details of each blend are discussed in Section III-A2. Each mixture was dry milled with 15 borosilicate beads (3 mm dia.) for 8–24 h to ensure thorough blending of the dust and iron oxides. Suspensions were prepared by mixing 3.3 g of the grime powder with 275 mL of acetonitrile (ReagentPlus grade, Sigma Aldrich).

B. Grime Application

Glass coupons were cut to 5.5 cm × 13 cm from 1.1-mm-thick low-iron Schott Borofloat glass (product number 03041085, Swift Glass). The selected glass is described by the manufacturer as having a lower density than soda lime glass and is highly transparent, making it suitable for PV applications. Tempered glass matching specific module types was not used due to the need to cut coupons to specific sizes. The dimensions were chosen to ensure that the coupon would fit within the contact points of a selected test cell. Each coupon was cleaned with commercial degreaser, which was followed by rinsing successively with tap water, distilled water, and ethanol (CDA 19 Denatured, Sigma Aldrich).

After cleaning, a dry coupon was weighed with a Mettler Toledo XP205 balance with 0.00001 g resolution and placed at a 45° angle inside a filtered spray chamber. The smoothest (nontin) face was oriented toward the sprayer to limit surface interaction effects. Coupons were coated by spraying the grime suspension in 25-mL aliquots with a high-velocity low-pressure automotive detailing gun (Transtar gravity-fed model 6618, 1.0-mm nozzle) held approximately 30 cm from the coupon surface. The detailing gun was aimed a few centimeters past the right edge of the coupon, and was slowly swept to the left until the spray plume had coated the entire coupon. The solvent was allowed to evaporate between coating steps. Dry samples were removed and weighed by difference to find the mass loading.

C. Optical Response Measurements

The optical response due to grime was measured using a 1-sun simulator, UV/vis/NIR spectrophotometer, and a quantum efficiency tester. Details of each measurement are discussed in this section, while comparisons are discussed in Section III-B. In order to evaluate the effects of grime on optical and electrical response, multicrystalline Si (mc-Si) cells ($\eta = 16\%$) were used to detect the light transmission through soiled slides. The PV response was measured using a Spectrolab XT-10 1-sun simulator that is equipped with a 1-kW Xenon lamp, producing an AM 1.5 spectrum. Calibrated HP 3458A multimeters were used for independent current and voltage measurements. An 81.25-cm^2 cell was centered on the temperature-controlled vacuum chuck, and test coupons were placed directly over the cell. Illumination from the simulator lamp was measured with a calibrated PRC Krochmann RS1 Si reference cell following each *I–V* sweep of the test cell.

Following the 1-sun test, the coupons were then subdivided into three 4.5-cm sections to fit into the sample chamber of a Varian Cary 5000 UV/vis/NIR spectrophotometer. These subcoupons were used for all subsequent spectroscopic measurements. The spectral response was evaluated by UV/vis/NIR spectroscopy from 300 to 1200 nm using three complimentary methods. Diffuse transmission and reflectance measurements

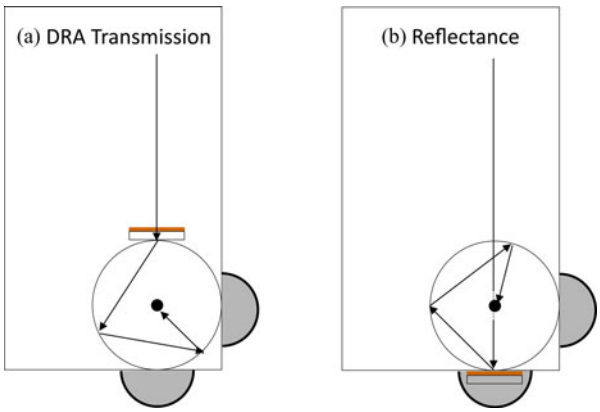

Fig. 1. Top-down schematic of samples placed in (a) DRA transmission and (b) reflectance configurations in the UV/vis/NIR spectrometer. (a) In the transmission mode, the sample beam passes through the grime layer and glass subcoupon into the integrating sphere and is eventually reflected to the detector at the base of the sphere. (b) In the reflectance mode, the sample beam passes through the integrating sphere to the grime surface and is reflected around the integrating sphere until it reaches the detector at the base. Any transmitted light passed through the subcoupon into a light trap.

were collected using a DRA-2500 diffuse reflectance accessory equipped with an integrating sphere. Transmission measurements were made by placing the coupon in front of the integrating sphere (see Fig. 1). Reflectance measurements were collected by placing the coupon behind the integrating sphere with the soiled face toward the chamber.

Direct transmission was collected through the standard double-beam holder with a clean piece of glass used in the reference cell to account for the spectral properties of the glass itself. All measurements were collected with 1-nm resolution in the UV/vis range (300–800 nm) and 4-nm resolution in the NIR range (800–1200 nm). The UV/vis scan rate was 600 nm/min and the NIR scan rate was 2400 nm/min. The slit bandwidth was fixed at 3 nm for UV/vis, while the NIR energy was set at 10.

Quantum efficiency measurements were collected by placing test subcoupons over an mc-Si cell in a PV Measurements QEX10. Three readings per wavelength were taken with a 0.5-s sampling interval at 10-nm increments from 300 to 1100 nm. The stage temperature was controlled to 25 °C, and the height was adjusted to 20.6 cm in order to focus the sample spot to fit within the cell crossfingers. The spectral response was recorded at a single point for each cell, without using a bias light.

III. Results and Discussion

A. Soil Types

Previous work [2] demonstrated a strong transmission dependence upon light absorbing (soot and carbonaceous material) compared with diffracting (quartz sand) materials. In this study, the grime formulation has been expanded to include spectrally responsive materials commonly found in regions throughout the U.S. southwest.

1) Identification: It is important to note that the work described herein focused on the spectral performance of artificially soiled PV cells, and thus, the color profile of each sample was replicated by comparatively simple combinations of common soil pigments in ratios of 40 wt% pigment to 60 wt% base grime blend. Pigment composition was designated as a range between red Fe_2O_3 (noted as 40:0) and yellow göthite (0:40), and combinations thereof, described as (Fe_2O_3: göthite). As noted by Torrent and Barrón [13], color and particle size are difficult to deconvolute; therefore, for simplicity, this study focused on the spectral response of various ratios of the same raw components (test dust, soot, and iron compounds). The morphology of grime particulates and the resultant patterning on PV surfaces will be the subject of a subsequent study.

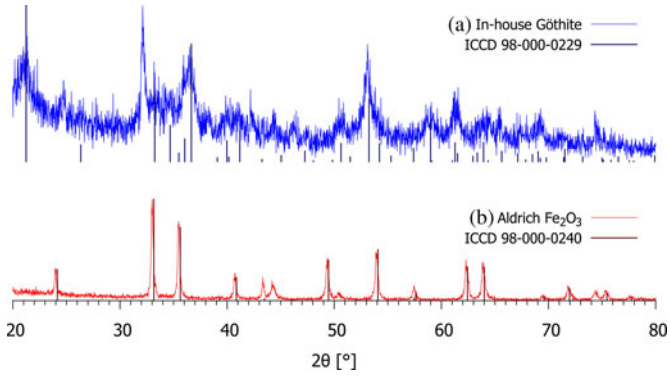

Fig. 2. XRD spectra of (a) synthetic and (b) commercial iron oxide powders.

2) Formulation: Grimes were formulated to match a range of red to yellow hues as discussed in the previous section. The overall color profile of the soil is due to a combination of reflectance and absorbance, which was replicated by mixing sand (diffracting medium) with soot (absorbing medium) and iron oxides (spectrally responsive media). Previously, we used several blends of AZ road dust and soot, with the minimum ratio of 3 wt% soot and 97 wt% sand [2]. However, iron-rich soils naturally contain little organic matter [12], [15]. Therefore, the soot, a strongly absorbing component, was reduced to less than 1 wt% in this paper. A range of colors was selected to correspond within the extrema of Munsell color swatch 10YR (yellow soil, observed in calcid soils in California, Arizona, New Mexico, and Texas) to 2.5YR (red soil, observed in psamment soils in California, Arizona, and Florida). In order to ensure consistency between batches of synthesized grime, trial batches were developed to determine the amount of pigment necessary to obtain suitable matches to these color swatches. A mass loading of 40 wt% göthite was found to replicate the 10YR swatch well. Therefore, 40 wt% pigment was used throughout the entire test series, and the color of each formulated blend (10:30, 30:10, and 40:0) was recorded. We emphasize that an exact color match of a specific soil was not an aim of this study. Rather, we have used a controlled series of soil simulants to demonstrate potential spectral effects due to the accumulation of common desert soils.

Where possible, NIST-traceable components were used as described previously [2]. Iron oxides were sourced commercially or prepared following standard methods [14]. During synthesis, some black particulates were noted, but due to the poorly crystalline (see Fig. 2) quality of the powder, identification of

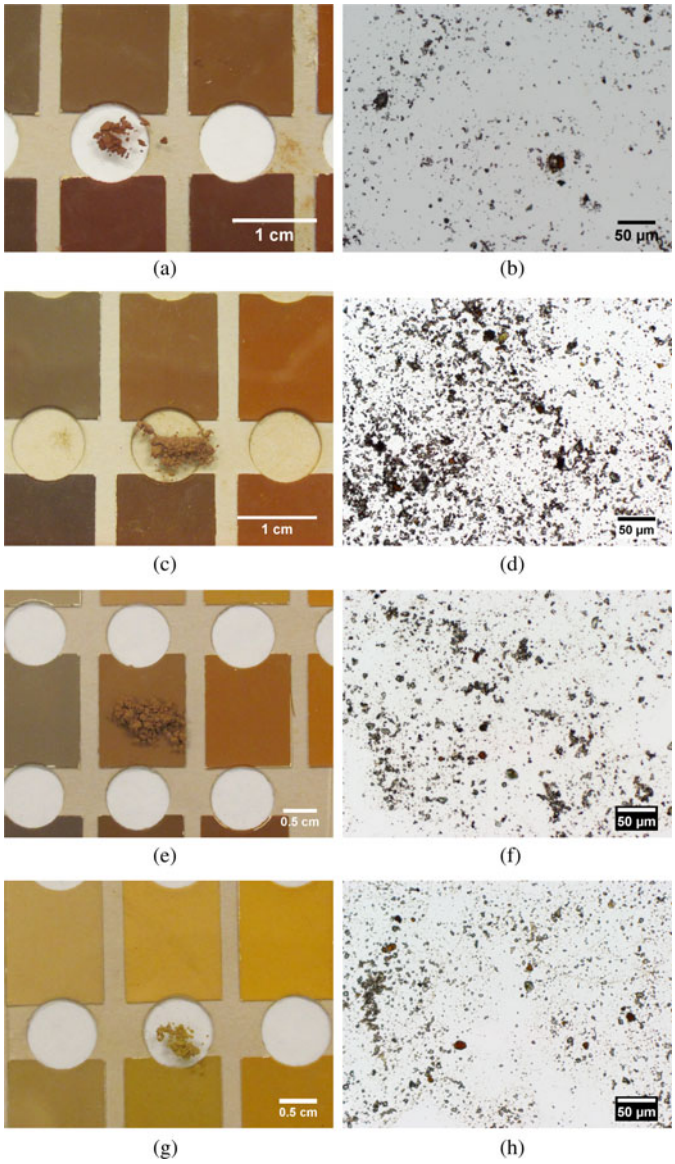

Fig. 3. Synthesized grime blends overlaid against Munsell color swatches. Each swatch card is identified by a hue (e.g., 10R) and specific color chip listing value and chroma (e.g., 3.5/3). Representative optical micrographs of coated coupons show the as-applied particulates. (a) 40:0, 10R 3.5/3. (b) Micrograph of 40:0. (c) 30:10, 2.5YR 3.5/4. (d) Micrograph of 30:10. (e) 10:30, 7.5 YR 5/4. (f) Micrograph of 10:30. (g) 0:40, 10YR 6/6. (h) Micrograph of 0:40.

minor components was not always feasible. In one instance, metallic iron impurities were found. When this batch was milled to generate 0:40 grime, a green-colored material matching swatch 5Y 5.5/3 was produced [8]. This color was well outside the test range, and the sample was not used. We note that since göthite was not available as a commercial or standard reference material, additional diligence was necessary to ensure that the samples were uniform across multiple batches. Subsequent batches produced consistent material, as only minor deviations from the desired Munsell swatch were noted from batch to batch. The as-deposited grime films are shown in Fig. 3.

B. Optical Response of Soil Types

The overall influence of different soil types on the performance of PV cells was evaluated with several complimentary methods. General performance loss was evaluated with a 1-sun simulator, while specific responses due to spectral interactions were recorded using a quantum efficiency tester and UV/vis/NIR spectrometer. In prior work [2], comparisons between the QE and UV/vis/NIR measurements were made by a simple ratio at a single wavelength. Since the components used in that study were not spectrally responsive, single-wavelength comparisons were a useful tool. This paper considers spectral effects, requiring analysis of the integrated response instead of a single wavelength. The spectral function $(S(\lambda)) = \mathrm{QE}(\lambda)$ or $\%T(\lambda))$ was integrated in the active range of the cell (300–1100 nm) and compared with the integral of the response of a clean coupon (1). An analogous calculation was undertaken for reflectance, which increased relative to the clean coupon, as shown in (2). The ratio between integrated areas was used to compare the normalized response among different instruments. The intensity of the incident light was taken into account by instrumental correction prior to each test.

$$\mathrm{Loss} = \frac{\int_{300}^{1100} S_{\mathrm{clean}}(\lambda)\mathrm{d}\lambda - \int_{300}^{1100} S_{\mathrm{soiled}}(\lambda)\mathrm{d}\lambda}{\int_{300}^{1100} S_{\mathrm{clean}}(\lambda)\mathrm{d}\lambda} \quad (1)$$

$$\mathrm{Gain} = \frac{\int_{300}^{1100} R_{\mathrm{soiled}}(\lambda)\mathrm{d}\lambda - \int_{300}^{1100} R_{\mathrm{clean}}(\lambda)\mathrm{d}\lambda}{\int_{300}^{1100} R_{\mathrm{clean}}(\lambda)\mathrm{d}\lambda}. \quad (2)$$

Loss was used as a performance indicator to quantitatively compare the effect of soiling on the reduction of the transmitted light reaching the cell and, ultimately, the reduction of energy collected from the device. The overall reduction in 1-sun performance, QE, and transmission was consistent for each grime type, as shown in Figs. 4(b), 5(b), and 6(b). In general, grime blends containing red Fe_2O_3 pigment tended to cause a greater overall loss than yellow, göthite-rich grime. A similar effect has been reported by Torrent *et al.* [12] as a tendency for hematite (Fe_2O_3) to mask the color of göthite in visual and spectroscopic measurements.

Reflectance measurements were also collected, but could not be directly compared with the previously mentioned transmission methods. The accumulation of particulates decreases the light transmission; therefore, the measurements discussed previously are lower than the clean coupon used as a baseline. In contrast, reflection measurements of soiled coupons increased relative to the baseline since grime particles are more reflective than the glass surface. Since the baseline reflectance was very low, these small increases (2) due to applied grime result in a large percentage gain [see Fig. 8(b)]. The work by Levinson *et al.* [9] has discussed the difficulty of studying the scattering effect of natural soil on opaque surfaces. We likewise find that, while reflectance follows a general trend, it was not possible to distinguish one grime type from another based on this measurement alone. Reflectance losses due to soil accumulation on parabolic or flat-plate mirrors for CSP applications would likely provide a much more distinct signal.

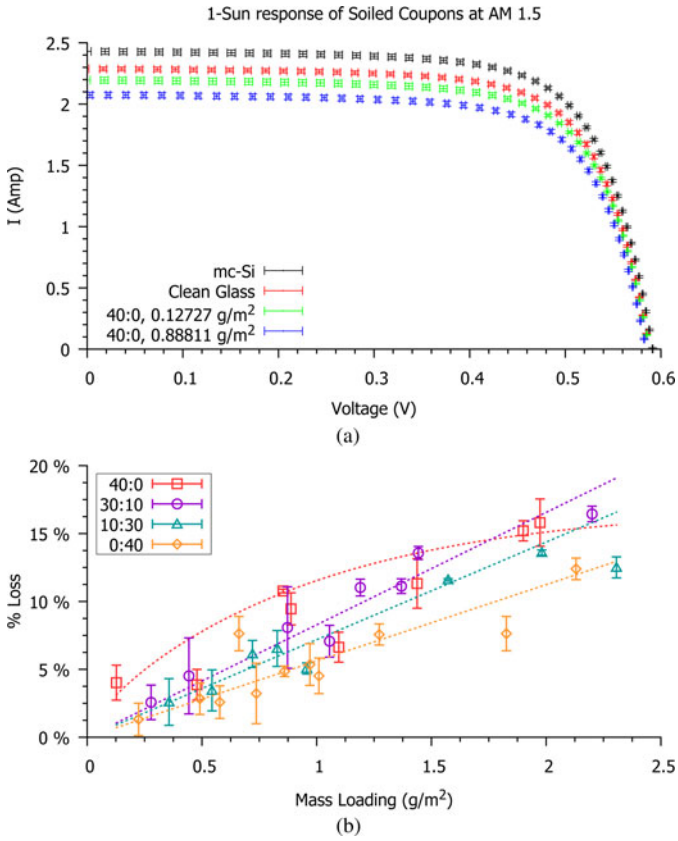

Fig. 4. (a) Representative *I–V* curves of polycrystalline Si (solid black) under clean (solid red) and 40:0 grime-soiled coupons (blue and green). (b) Comparison of response among each soil type fit to linear (30:10, 10:30, and 0:40) and error function fits (40:0). Reprinted from [8].

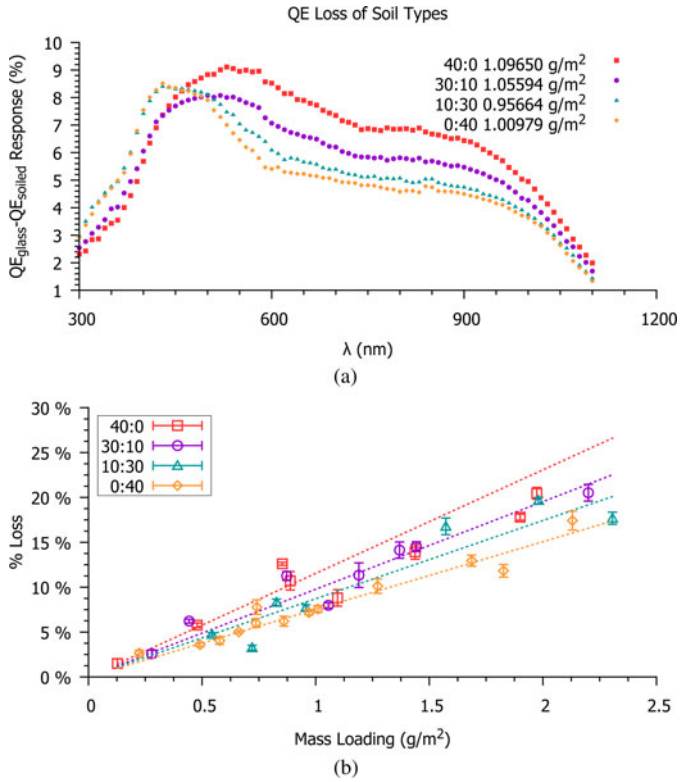

Fig. 5. (a) Comparison of QE polycrystalline Si under glass coupons coated with a range of soil types. Blends rich in göthite (10:30 and 0:40) exhibit a narrower peak at 425 nm. (b) Integrated response and linear fits of each soil type. Reprinted from [8].

1) AM 1.5 Irradiance: A 1-sun simulator was used to find the full-spectrum response of the entire cell shaded by a glass coupon with various loadings of grime. The entire surface of the cell was covered by a grime-coated coupon and subjected to ten repeat tests, which were averaged to produce the representative curves shown in Fig. 4(a). As in previous work [2], the coupon was not optically or mechanically coupled to the underlying cell, allowing for subsequent tests in other instruments. Optical coupling is a significant consideration for assembled modules; however, the goal of this study was to correlate the response of several measurement techniques. This comparison provided the necessary data to evaluate the significance of grime color to the overall cell performance and insight into the specific optical properties that influence performance.

The percent difference between the measured $I_{\rm sc}$ of the test coupon and a clean reference was used to compare coupons with various grime types and mass loading. The grime coating caused a pronounced decrease in $I_{\rm sc}$ [see Fig. 4(a)]; however, the fill factor and $V_{\rm mp}$ were unaffected. These observations of a single cell contrast with those of Gostein *et al.* [16], who investigated natural soiling over large arrays of modules. In addition to a substantial loss in the power output and $I_{\rm sc}$, they observed a change in shape of the *I–V* curve. In the literature study, uneven shading throughout the module and string caused power decreases in the module, which have no analog in the present cell tests. A thorough understanding of the per-mass loss of each cell could be used as a baseline to model larger modules, and adapted as necessary to incorporate variable shading.

The decrease in $I_{\rm sc}$ as a function of mass loading was found for each grime type. These data were expressed as a percentage of the reference condition [see Fig. 4(b)] and compared with the integrated losses in Figs. 5(b) and 6(b). All three measurements show a similar trend where red, Fe_2O_3-rich grime causes a greater decrease than yellow grime. The 40:0 response was not linear within the range of collected data.

2) Quantum Efficiency: Quantum efficiency scans were collected from 300 to 1100 nm using a coupon overlaid on an mc-Si cell. Grime mixtures rich in Fe_2O_3 tended to have broad responses, with the greatest loss corresponding approximately to the peak solar spectrum [see Fig. 5(a)]. In contrast, göthite-rich samples (10:30 and 0:40) showed a much more pronounced, less broad peak at 425 nm. This peak corresponds to similar features observed in transmission (see Fig. 7) and reflectance [see Fig. 8(a)] measurements. When compared with other measurements [see Figs. 6(a) and 8(a)], this feature is most likely due to absorption in this narrow (albeit high-energy) region. Overall, the measured loss due to yellow grime is less than red grime [see Fig. 5(b)] when integrated over all wavelengths.

3) UV/vis/NIR: Quantitative spectral responses for each soil type were found by UV/vis/NIR spectroscopy. Transmission and reflectance features in the UV, visible, and near infrared region

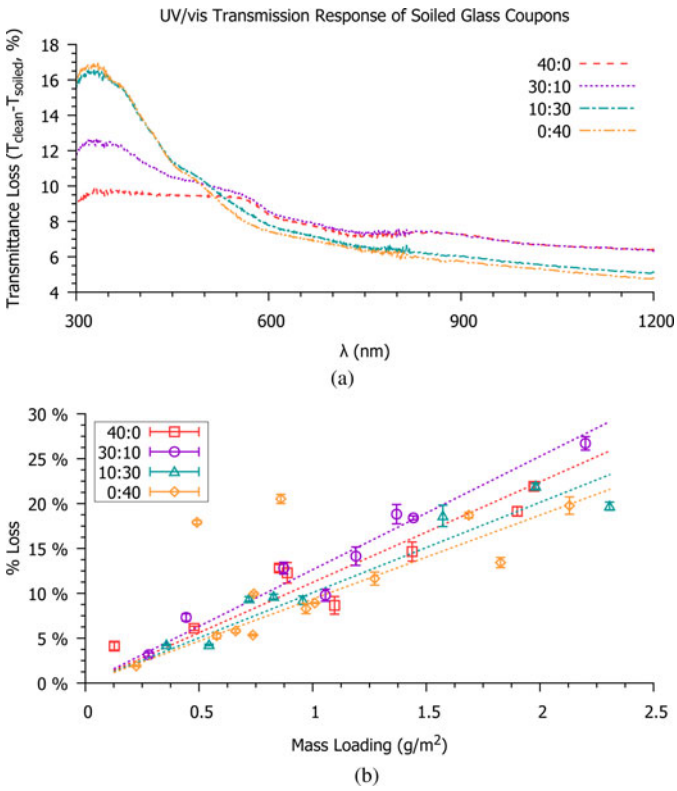

Fig. 6. (a) DRA loss spectra of soil types between 0.95- and 1.0-g/m^2 mass loading. (b) Linear fits to integrated responses. Reprinted from [8].

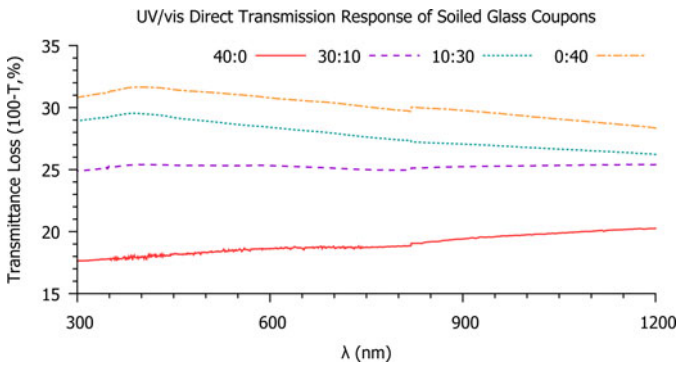

Fig. 7. Direct transmission UV/vis/NIR spectra of 40:0, 30:10, 10:30, and 0:40 type soils between 0.95 and 1.0 g/m^2 mass loading.

were investigated to determine effects on the total transmission loss and decreases at specific wavelengths.

a) DRA transmission: Diffuse transmission (noted as DRA for the diffuse reflectance accessory) was measured by replacing the standard sample holder with an integrating sphere. The grime-coated coupon was mounted directly in front of the integrating sphere in a single-beam configuration, as illustrated in Fig. 1. This configuration enabled the collection of the direct and diffuse light but does not account for the angle of incidence.

The shape of the 40:0 spectrum closely matched the clean coupon, except over the range between 600 to 900 nm. This is most likely due to reflection [see Fig. 8(a)] of the red light. Wavelength-dependent losses through this grime were minimal, leading to a neutral density filter effect that is described in Section III-C. Grime blends containing göthite showed a much greater deviation from the clean coupon. A large peak is centered at 350 nm, as well as a shoulder from 450 to 550 nm [see Fig. 6(a)]. The shoulder may be a smeared artifact of the peak found at 435 nm in the literature [11]. Both features may be due to light scattering through the grime layer and interacting with the glass, as discussed in Section III-C.

b) Direct transmission: Direct transmission was collected by using the standard double beam configuration in the UV/vis/NIR spectrophotometer, where a clean coupon was placed in the reference position prior to collecting a baseline scan, thus eliminating the response of the glass. Since this measurement was restricted to direct transmission, it was not compared with the other techniques that utilized both the direct and diffuse light. The resulting profiles showed significant responses in the visible (see Fig. 7) region dependent on grime composition. Grime-coated coupons that were rich in Fe_2O_3 (40:0 and 30:10) exhibited a slow increase in measured loss as a function of wavelength, with no significant peaks. Göthite-rich blends (10:30 and 0:40) exhibited a loss peak at 425 nm and steadily decreased thereafter. A general trend was observed over the range of all samples, in which göthite content correlated with the decrease in transmission.

c) Reflectance: Reflectance measurements [see Fig. 8(a)] likewise showed a significant response in the visible and NIR regions. The 40:0 grime exhibited a peak at 600 nm, which roughly corresponds to the 575 nm reported in the literature for Fe_2O_3 [11]. The 0:40 grime exhibited prominent göthite peaks at 425 (435 nm in the literature [11]) and 535 nm; however, the NIR response was substantially reduced as compared with the Fe_2O_3-containing soils. Göthite-containing grime also caused the reflectance to *decrease* below the value of the clean glass [see Fig. 8(a)] between 300 and 400 nm. Since the light is not forward-scattered (see Fig. 6), it is either absorbed by the göthite or scattered in the plane of the film. This may have significant device implications, as discussed in Section III-E. The 30:10 and 10:30 grime-coated coupons exhibited a blend of features common to both göthite and Fe_2O_3. While reflectance measurements were not as easily quantifiable as the 1-sun, QE and DRA transmission results, the trend between each of the spectra best illustrates the significance of light scattering due to the range of grime types.

C. Comparison of Methods

An essential aspect of this paper is to compare the optical properties of a range of typical spectrally responsive soils with the corresponding decreases they may cause in the PV device performance. Since the 1-sun simulator includes all relevant wavelengths, the data can be compared with the other integrated monochromatic measurements. The integrated response of each of the QE and 1-sun tests are plotted against %DRA transmission in Fig. 9. Note that these data are from Figs. 4(b), 5(b), and 6(b). These figures highlight a consistent trend in which the data from each grime type correlate well. When evaluated as a function of mass loading, Fe_2O_3-rich grime caused a greater decrease in the

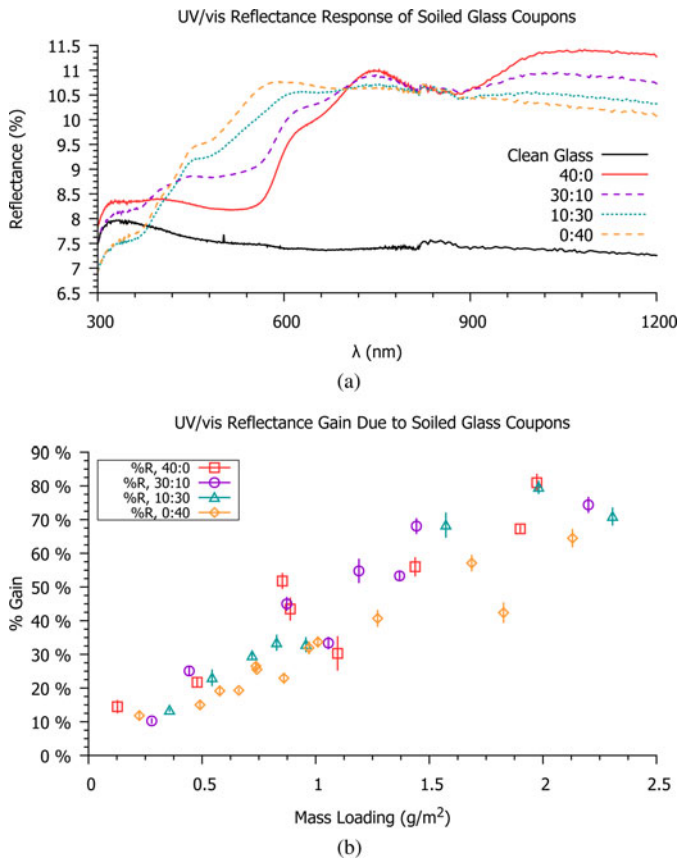

Fig. 8. (a) Reflectance spectra of soil types between 0.95 and 1.0 g/m^2 mass loading. A clean glass reference coupon spectrum is shown in solid black. (b) Integrated results shown as an increase relative to clean glass.

device response [see Figs. 4(b), 5(b), and 6(b)] than göthite-rich grime.

The physical mechanism for this behavior can be understood by examining the spectral behavior of each grime type. The red Fe_2O_3 grime blends function as a neutral density filter to direct the incident light, as is best illustrated by the nearly featureless curves in Fig. 7. Yellow göthite-rich grime scatters light as demonstrated by the pronounced 425-nm peaks in Figs. 5(a), 6(a), and 7. Despite the strong peak, much of the scattered light may still reach the underlying cell, thus reducing the overall impact of yellow soil [see the comparisons in Figs. 4(b), 5(b), and 6(b)]. This effect is most pronounced for the 0:40 spectra. A strong peak was observed in the DRA spectra [see Fig. 6(a)] compared with direct transmission (see Fig. 7). The reflectance spectrum decreased below the reference within this same region [see Fig. 8(a)]. These features suggest that the incident light is lost either by absorption or evanescent reflection between the grime and glass interface. Since the direct transmission peak is centered around 400 nm, it is reasonable to conclude that scattering is a significant contributor to the optical properties of göthite-rich soil. Despite these strong features in a narrow wavelength band, the integrated response due to 0:40 grime was consistently lower than any other grime.

The increase in reflectance was too loose to discern a significant trend among each of the four grime types [see Fig. 8(b)].

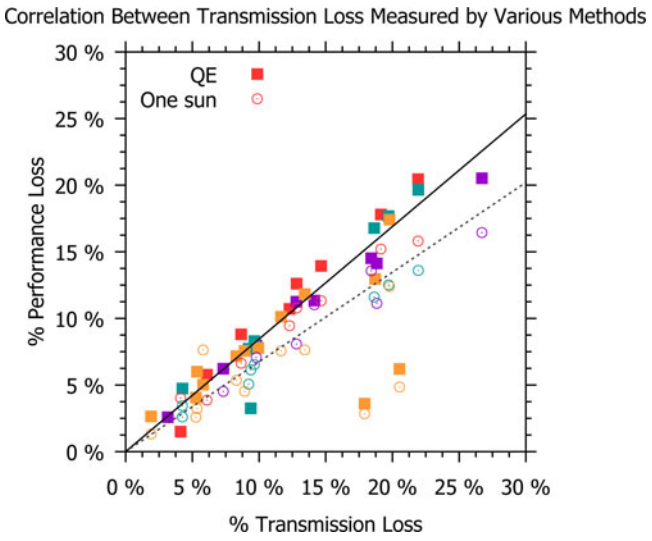

Fig. 9. Comparison of QE (■) and 1-sun (⊙) integrated losses as a function of transmission. Both measurements show good correlation with the measured %DRA transmission. Outliers near 20% transmission loss are not included in the curve fits but are shown for completeness.

A similar upward trend was observed for all soil types, but the calculated loss between points can vary by as much as $\sim 40\%$. Since the reflectance of clean glass is small, any increase in the reflected light due to grime results in a large percentage change. For the same reason, it is difficult to correlate the absolute change in reflection with measured changes in transmission.

Therefore, the best comparisons are among devices that collect both the direct and diffuse light, including the 1-sun tester, UV/vis/NIR DRA spectrometer, and QE test stand. Additionally, the device response may introduce an internal sensitivity to göthite-rich soil, as illustrated by a comparison of the QE [see Fig. 5(a)] and DRA [see Fig. 6(a)] spectra. While the peak location is similar between the two devices, the QE captures the combined response of the PV device behavior and the optical properties of grime. In contrast, the DRA more clearly demonstrates the pure optical properties of the grime. The broad response of the QE to predominately red soil types suggests that the selected cells are not spectrally sensitive to this grime type to the same extent of the calibrated photodiodes in the UV/vis/NIR spectrophotometer. PV cells are not designed to respond to sharp transitions in the spectrum; therefore, any effect of the grime is averaged over a broader wavelength. It is therefore useful to collect data from a range of test instruments to fully understand the implications of soil accumulation.

D. *Data Analysis and Repeatability*

Grime coatings below 1 g/m^2 are consistent for all tested grime types and caused a $\sim$10% reduction in the light captured by each respective test device. A similar study by Al-Hasan [17] reported a critical mass loading from 10 to 100 g/m^2 at various wavelengths due to reddish-brown soil applied to glass. The order of the magnitude difference between the literature and this paper may be due to substantial variation in the application techniques that are used. Al-Hasan's technique is representative

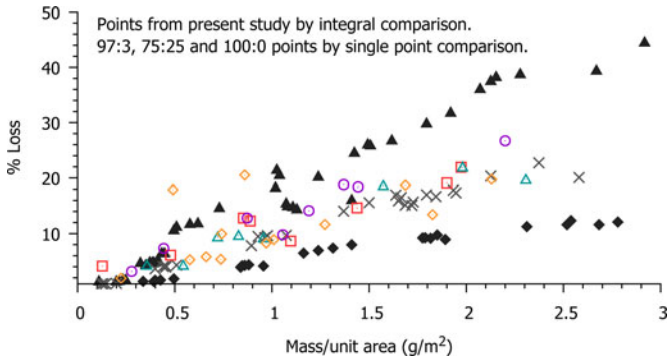

Fig. 10. Comparison of %T data with the results from prior work [2]. Dark filled symbols denote the pure sand (♦) and 25 wt% soot: 75 wt% sand (▲) data from prior work. The 3 wt% soot: 97 wt% sand blend is shown by (×). Note that prior data were collected as a single point percentage at $\lambda = 630$ nm, while this study is reported as an integrated area (1).

of dust deposition during a wind storm, while the technique presented here represents a slower aerosol deposition mode. The variations may indicate a correlation with the particle size, in which small particulates, similar to those used in this study, obscure more area than a similar mass (but substantially smaller volume) of large wind-blown particulates. The present results for loss as a function of mass loading roughly fall within the range established in prior work [2]. It should be noted that earlier work used single-point comparisons at 630 nm, not integral data as used in this paper. Each pigmented grime blend in this paper caused a greater deviation than a similar mass loading of pure AZ test sand but below the urban analog with 25 wt% soot in the earlier study (see Fig. 10). This comparison emphasizes a critical aspect to accelerated soiling studies. The spectral effects of each desert-like pigment (40:0, 30:10, etc.) exhibit a noticeable trend when compared with each other, but are overshadowed when compared with urban grime. Tailoring the composition of test grime for specific installations would require a balance between the development cost and accuracy. Broad generalizations can be made by using simple soil analogs; however, more region-specific formulas require greater investment in identifying and incorporating relevant components. The level of accuracy needed must be balanced with the complexity of the grime analogue and intended technology (i.e., flat plate or CPV).

E. Device-Specific Implications

A loose trend among the various measurement types suggests that Fe_2O_3-rich grime blends interfered with the light transmission more than göthite-rich grime [see Figs. 4(b), 5(b), and 6(b)]. Each measurement technique indicated that 40:0 or 30:10 grime caused the greatest decrease in integrated response. Interestingly, the 30:10 soil extrapolates to a slightly greater response than the 40:0 in the DRA test [see Fig. 6(b)]. Since the DRA uses a calibrated detector rather than a multicrystalline PV cell, it is more sensitive to wavelength variations than the QE or 1-sun tests. This effect is illustrated in Figs. 5(a) and 6(a). In Fig. 5(a), the quantum efficiency of the underlying mc-Si cell dominates the measured response between 350 and 450 nm. In comparison, the DRA [see Fig. 6(a)] shows a much more significant response between the grime types in this range. The curve for 30:10 grime can be seen to be a numerical combination of the 40:0 and 0:40 responses. Above 600 nm, the Fe_2O_3 dominates the response, and the 30:10 and 40:0 curves overlap. Below 600 nm, the behavior of the göthite begins to dominate, resulting in a greater total transmission loss than either the 40:0 or 0:40 grime. Since the mc-Si detector used for the QE scan is not as sensitive in the sub-400-nm range as the DRA detector, this behavior is not observed. For practical use, this suggests that PV devices with a stronger blue response, such as CdTe (300–900 nm [18]), would be more sensitive to yellow soils, while CIGS cells (400-1100 nm [18]) would be more sensitive to red soils.

For very wavelength-specific devices, such as multijunction cells, göthite-rich soils may be more detrimental to performance. Although the integrated response is greatest for 40:0 grime, the strongest individual peaks are due to 0:40 grime between 350 and 450 nm. If a diode layer operating in this range collected less light, the limiting current would affect each of the remaining layers in series. A decrease in the available blue spectrum light may have a greater impact on the remaining cell layers and reduce the output of the entire device. In a recent review, Baig *et al.* [19] discussed the effects of both nonuniform irradiance and chromatic aberration on CPV systems. Soil composition and necessary cleaning schedules should be considered for these systems. Additionally, as Wohlgemuth *et al.* [20] noted, nearly all glass manufacturers have stopped using ceria as a UV-blocking additive in PV cover glass. These newer systems may be more sensitive to the effects of yellow soils. Therefore, optical properties of an obscurant film cannot independently be used as an estimate for the overall power loss without consideration of the underlying PV device.

IV. Conclusion

Artificial grime mixtures can be synthesized to simulate the range of color profiles corresponding to common soils. The variation between each grime composition was detectable by complimentary methods between different instruments. The 1-sun simulator provided the most applicable measurements to fielded systems, i.e., *I–V* curves. When compared with spectral data from the UV/vis/NIR and QE instruments, the magnitude of the responses agreed well between the three techniques. Reflectance and direct transmission measurements were not easily comparable due to fundamental differences in the physics of the measurements. The information gleaned from reflectance and direct transmission measurements is useful to understand spectral properties of various soils, whereas 1-sun, QE, and DRA transmission measurements can be used as complimentary techniques to measure spectrally sensitive losses.

Red, Fe_2O_3-rich grime functioned as a nearly neutral density filter for direct (normal) irradiance. Yellow göthite-rich grime scattered the light, causing pronounced peaks in the spectrum. This forward scattering made the yellow grime less detrimental to the overall performance than red grime. Specific responses due to mineral content were identified in the diffuse scattering

and reflectance spectra. The yellow grime obscured more light in the blue region of the spectrum, which may be particularly important to multijunction cells and CPV systems. The potential loss that is experienced by nonspectrally sensitive devices, such as mc-Si, may not require a location-specific test grime. The spectral response due to accumulated soil should be considered for spectrally sensitive CPV systems, as well as in regions where high mass loadings are expected. Efforts to correlate naturally occurring soils with specific laboratory test grime blends and relevant devices are currently underway.

ACKNOWLEDGMENT

The authors would like to thank J. Kratochvil, D. Riley, and C. Robinson for helpful discussions.

REFERENCES

[1] T. Sarver, A. Al-Qaraghuli, and L. L. Kazmerski, "A comprehensive review of the impact of dust on the use of solar energy: History, investigations, results, literature, and mitigation approaches," *Renewable Sustainable Energy Rev.*, vol. 22, pp. 698–733, 2013.

[2] P. D. Burton and B. H. King, "Application and characterization of an artificial grime for photovoltaic soiling studies," *IEEE J. Photovoltaics*, vol. 4, no. 1, pp. 299–303, Jan. 2014.

[3] S. R. Cattle, K. Hemi, G. L. Pearson, and T. Sanderson, "Distinguishing and characterising point-source mining dust and diffuse-source dust deposits in a semi-arid district of eastern Australia," *Aeolian Res.*, vol. 6, pp. 21–29, 2012.

[4] S. Biryukov, D. Faiman, and A. Goldfeld, "An optical system for the quantitative study of particulate contamination on solar collector surfaces," *Sol. Energy*, vol. 66, no. 5, pp. 371–378, 1999.

[5] J. A. Macko, R. R. Lunt, T. P. Osedach, P. R. Brown, M. C. Barr, K. K. Gleason, and V. Bulovic, "Multijunction organic photovoltaics with a broad spectral response," *Phys. Chem. Chem. Phys.*, vol. 14, pp. 14 548–14 553, 2012.

[6] G. A. Landis, "Dust obscuration of mars solar arrays," *Acta Astronautica*, vol. 38, no. 11, pp. 885–891, 1996.

[7] J. K. Kaldellis, P. Fragos, and M. Kapsali, "Systematic experimental study of the pollution deposition impact on the energy yield of photovoltaic installations," *Renewable Energy*, vol. 36, no. 10, pp. 2717–2724, 2011.

[8] P. D. Burton and B. H. King, "Artificial soiling of photovoltaic module surfaces using traceable soil components," presented at the IEEE 39th Photovoltaics Spec. Conf., Tampa, FL, USA, 2013.

[9] R. Levinson, P. Berdahl, A. Asefaw Berhe, and H. Akbari, "Effects of soiling and cleaning on the reflectance and solar heat gain of a light-colored roofing membrane," *Atmosph. Envir.*, vol. 39, no. 40, pp. 7807–7824, 2005.

[10] W. Einfeld, R. M. Boucher, M. S. Tezak, M. C. Wilson, and G. S. Brown, "Evaluation of surface sampling method performance for bacillus spores on clean and dirty outdoor surfaces," Sandia Nat. Labs., Albuquerque, NM, USA, Tech. Rep. SAND2011-4085, 2011.

[11] R. Arimoto, W. Balsam, and C. Schloesslin, "Visible spectroscopy of aerosol particles collected on filters: Iron-oxide minerals," *Atmosph. Envir.*, vol. 36, no. 1, pp. 89–96, 2002.

[12] J. Torrent, U. Schwertmann, H. Fechter, and F. Alferez, "Quantitative relationships between soil color and hematite content," *Soil Sci.*, vol. 136, no. 6, pp. 354–358, 1983.

[13] J. Torrent and V. Barrón, "The visible diffuse reflectance spectrum in relation to the color and crystal properties of hematite," *Clays Clay Miner.*, vol. 51, no. 3, pp. 309–317, 2003.

[14] U. Schwertmann and R. M. Cornell, *Iron Oxides in the Laboratory Preparation and Characterization*, 2nd ed. Hoboken, NJ, USA: Wiley-VCH, 2000.

[15] C. Pizarro, M. Escudey, and J. Fabris, "Influence of organic matter on the iron oxide mineralogy of volcanic soils," *Hyperf. Interact.*, vol. 148–149, no. 1, pp. 53–59, 2003.

[16] M. Gostein, B. Littmann, J. R. Caron, and L. Dunn, "Comparing PV power plant soiling measurements extracted from PV module irradiance and power measurements," presented at the IEEE 39th Photovoltaics Spec. Conf., Tampa, FL, USA, 2013.

[17] A. Y. Al-Hasan, "A new correlation for direct beam solar radiation received by photovoltaic panel with sand dust accumulated on its surface," *Sol. Energy*, vol. 63, no. 5, pp. 323–333, 1998.

[18] H. Qasem, T. R. Betts, H. Mllejans, H. AlBusairi, and R. Gottschalg, "Dust-induced shading on photovoltaic modules," *Progr. Photovoltaics: Res. Appl.*, vol. 22, pp. 218–226, 2012.

[19] H. Baig, K. C. Heasman, and T. K. Mallick, "Non-uniform illumination in concentrating solar cells," *Renewable Sustainable Energy Rev.*, vol. 16, no. 8, pp. 5890–5909, 2012.

[20] J. H. Wohlgemuth, M. D. Kempe, and D. C. Miller, "Discoloration of PV Encapsulants," presented at the IEEE 39th Photovoltaics Spec. Conf., Tampa, FL, USA, 2013.

Authors' photographs and biographies not available at the time of publication.